BOREAL ENVIRONMENT RESEARCH 23: 105–125
ISSN 1797-2469 (online)

Helsinki 4 April 2018

Sources and composition of particulate matter in boreal arctic environment next to an active mining area

Hilkka Timonen[1)]*, Kimmo Teinilä[1)], Minna Aurela[1)], Felipe Reyes[2)], Yeanice Vásquez[2)], Matthew Bloss[1)], Pedro Oyola[2)], Risto Hillamo[1)], Eija Asmi[1)] and Sanna Saarikoski[1)]

[1)] *Finnish Meteorological Institute, Atmospheric Composition Research, P.O. Box 503, FI-00101 Helsinki, Finland (*corresponding author's e-mail: hilkka.timonen@fmi.fi)*
[2)] *Centro Mario Molina Chile Ltda, Antonio Bellet 292, Oficina 602, Santiago, Región Metropolitana, Chile*

Received 23 Nov. 2017, final version received 12 Mar. 2018, accepted 13 Mar. 2018

Timonen H., Teinilä K., Aurela M., Reyes F., Vásquez Y., Bloss M., Oyola P., Hillamo R., Asmi E. & Saarikoski S. 2018: Sources and composition of particulate matter in boreal arctic environment next to an active mining area. *Boreal Env. Res.* 23: 105–125.

Detailed measurements of particulate matter (PM) were conducted in the boreal arctic environment, next to an actively-operating open pit mine. Three distinct PM sources with different chemical composition were identified: mining activities, long-range transported (LRT) PM and clean arctic air. The main sources of PM originating from the mining area were vehicular emissions for submicron particles (PM_1) and mining activities (including re-suspended dust) for supermicron particles (PM_{1-10}). PM_1 originating from mining activities had a high contribution of black carbon (44%–48%), organic carbon (31%–46%) and a minor contribution from inorganic ions (< 21%) suggesting that it was mainly originating from the vehicles. Based on elemental composition it is likely that supermicron particles were mechanically generated and re-suspended PM from mining activities. In contrast, for the air mass originating from the arctic areas, PM concentrations were very low and PM had a different chemical composition. During the LRT episode, elevated sulphate concentrations in submicron particles were observed.

Introduction

The anthropogenic particulate matter (PM) sources in sparsely populated arctic areas are scarce and particulate matter concentration typically very low (e.g. Lihavainen *et al.* 2015, Hienola *et al.* 2017). The mining industry has expanded especially in northern Finland in recent years. Mining and associated early refining processes release particulate matter into the air. Previous studies have shown that the main sources of particulate matter in the mines are the operations associated with deposit extraction (drilling, crushing, etc.), blasting and vehicular engine emissions (used in mining machines, ore hauling and for transportation of people) (Ghose 2007, Noll *et al.* 2007, Csavina *et al.* 2011, Aneja *et al.* 2012, Saarikoski *et al.* 2017). Dust from drilling and deposit extraction is moderately well known on the basis of previous studies (Ghose 2007, Csavina *et al.* 2011, Aneja *et al.* 2012, Gonzales *et al.* 2014). Contrary to dust, particulate matter

Editor in charge of this article: Veli-Matti Kerminen

emissions from the diesel vehicles operating in the mines consist mainly of sub-micrometer particles (e.g. Maricq 2007). Number concentrations and size distributions of submicron particles typically originating from the diesel vehicles have been studied in the mines, but the data on the particle chemical composition is limited and based on solely offline sampling with long averaging times (Noll *et al.* 2006, 2007).

In most cases, the mining emissions do not stay in the mining area but are transported outside and may cause undesirable effects on surrounding nature and on people living near mines or refining facilities (Pandey *et al.* 2014). For example, emitted dust can contain toxic metals that can deposit and accumulate in the ecosystems (Pandey *et al.* 2014). Arctic is known to be more sensitive to the changes in the atmospheric concentrations of pollutants and is also strongly affected by the climate change (Quinn *et al*. 2011). Mining in the vicinity of the Arctic and other snow and ice covered areas poses an additional climate threat due to the impact of deposited pollutants on the surface energy balance. Light-absorbing impurities (LAI), such as dust and soot particles, have been shown to decrease surface albedo, contributing to earlier snow and ice melting and leading to the changes in snow density and structure (Flanner *et al.* 2007, Meinander *et al.* 2014, Qu *et al.* 2014, Tedesco *et al.* 2016). These impurities are found in elevated concentrations near anthropogenic and industrial centers, including the mines (Schmitt *et al.* 2015, Khan *et al.* 2017, Schmale *et al.* 2017). LAI contribution to snow and ice melting can be dramatic in the areas where agriculture and drinking water depend on fresh-water glacier supplies, such as the Himalayas and the Andes (Bradley *et al.* 2006, Menon *et al.* 2010, Schmitt *et al.* 2015).

Exposure to PM may cause adverse effects on the environment and health and well-being of workers along with the population living nearby. Health influences are depending on source, composition and size of particles (Pope and Dockery 2006). Vehicular engine emissions are known to have adverse health effects and the World Health Organization (WHO) has classified diesel engine emissions carcinogenic (IARC 2012). Formation of mineral dust is mechanical and dust exists mainly in coarse particles (particles with mobility diameter $D_p > 2.5$ µm), but include also substantial amount of fine particles (particles with mobility diameter $D_p < 2.5$ µm). Fine particles are penetrating to the upper respiratory system and are causing negative health effects, such as silicosis (Thomas and Kelley 2010).

In order to understand and quantify the influences of particulate matter released by a mine on air quality, human health and climate, comprehensive measurements of PM emissions from mining activities are needed. This study characterizes the chemical composition and size distribution of PM in the close proximity of an actively operating open pit mine in Finnish Lapland. The aim of this study was to gain further understanding of the sources and processes affecting the PM concentrations in the vicinity of an open pit mine in an arctic area. This information can be used in further studies to determine the contribution of mining activities to local air quality, environment nearby and more widely to the Arctic climate change.

Experimental methods

Measurement location and setup

Particulate matter measurements were conducted from 23 April to 4 June 2014 next to the Kevitsa nickel-copper-platinum group elements (PGE) mine (67°41´44´´N, 26°56´31´´E) that is located approximately 142 kilometres northeast of Rovaniemi, Lapland (http://www.boliden.com/Operations/Mines/Kevitsa/). The mining at Kevitsa is carried out in an open pit (depth approximately 500 m). The Boliden Kevitsa mine started operation in 2012. Currently the Kevitsa mine has approximately 450 employees and around 7911 ktonnes of ore is processed annually (2017). The mined ore is hauled to nearby facility for processing. Ore processing is traditional. The mined ore is crushed in a primary crusher and the crusher product is screened to send the Autogenous Grinding (AG) mill media to stockpile, the mid product to secondary crushing and pebble storage for the pebble mill media. After that the crushed ore is ground in a combination of AG mills and a pebble mill. Copper and nickel ore is recovered

in separate flotation circuits, where products are being thickened and filtered in order to produce concentrates. Two concentrates are produced; the first being a Nickel-Copper-PGE-Gold concentrate with up to 12% nickel and a copper-PGE-gold concentrate with up to 28% copper. The Boliden Kevitsa is committed to adhere the Finnish Towards Sustainable Mining (TSM) Standard (prepared in 2016), that provides guiding principles for mining that are sustainable in terms of environmental, social and economic performance.

The measurements were conducted on the north-west side of the mine pit, next to the road that was used to haul ore from the pit for further processing. The distance from the edge of the pit to the measurement container was approximately 150 m providing an ideal location for the measurements of downwind emissions of mining activities. Weather variables (temperature, relative humidity, wind direction and wind speed) were measured continuously with the Vaisala Weather Transmitter WXT520 four meters above the roof of the measurement container. Weather during the measurements was typical for a late spring in the Arctic. At the beginning, temperature was often below 0 °C and it was snowing. At the end of the measurement period all snow had melted and temperature was between 10 and 20 °C. The prevailing wind direction was north during the campaign.

Aerosol instruments

Online aerosol composition measurements

The Aerodyne Time-of-Flight Aerosol Chemical Speciation Monitor (ToF-ACSM) is designed for the long-term monitoring of a submicrometer (50–800 nm) non-refractory aerosol composition i.e. organics, sulphate, ammonium, nitrate and chloride with high temporal resolution and medium mass resolution ($m/\Delta m$ up to 600, where m is the mass of the ion of interest and Δm is the peak width). The instrument is described in detail elsewhere (Fröhlich *et al.* 2013, Timonen *et al.* 2016). The ionization efficiency (IE) of the nitrate ions was determined with ammonium nitrate (NH_4NO_3) aerosol prior to the campaign. The IE for nitrate was 65 ions pg^{-1}. Other measured ions were calculated based on the $IE_{nitrate}$ using relative ionisation values of 4, 1.2, 1.4 and 1.3 for ammonium, sulphate, organics and chloride, respectively. The time resolution of 10 min (1 min filter background and 9 min ambient air with particles) was used in the measurements. Post-processing was performed using the data analysis package "Tofware" (version 2.5.2, www.tofwerk.com/tofware) running in the Igor Pro (Wavemetrics, OR, USA) environment.

The Multiangle Absorption Photometer (MAAP, Model 5012, Thermo Fisher Scientific) measures black carbon mass loadings based on aerosol optical absorption (Petzold *et al.* 2004). The MAAP was specifically developed to reduce the uncertainties in black carbon measurements caused by aerosol scattering. The reduction of light transmission, multiple reflection intensities, and air sample volume are continuously integrated over the sample run period to provide a real-time data output for the absorption coefficient at wavelength 637 nm (Müller *et al.* 2011), which is converted to equivalent black carbon concentrations assuming a value of 6.6 $m^2\ g^{-1}$ for the mass absorption cross section.

Online aerosol size distribution measurements

Number size distribution of particulate matter was measured using a Scanning Mobility Particle Sizer (SMPS) and an Aerodynamic Particle Sizer (APS). The SMPS (Wang *et al.* 1990) consists of a Differential Mobility Analyser (DMA, model 3081) coupled to electrostatic classifier (model 3080) and a Condensation Particle Counter (CPC, TSI model 3776). The DMA classifies particles to different size bins based on their electrical mobility. The number concentration of particles in each size bin is subsequently measured with a CPC. The size range of the SMPS measurements was 10–415 nm (D_p, particle mobility diameter) with aerosol flow of 1.5 liters per minute (LPM) and sheet flow of 6 LPM. Time resolution of the size distribution measurement was three minutes.

The APS (TSI Model 3321, Peters *et al.* 2003) was used to measure the number size

distribution of particles with aerodynamic diameters, D_a, above 0.5 µm. A sample flow of 1 LPM and sheet flow of 4 LPM were used. The APS is a spectrometer that measures aerodynamic particle diameter based on particle time of flight in an accelerated flow field. The nominal particle size range of the APS was 0.5–20 µm. For the APS the counting efficiency of particles drops quickly below 1 µm, and particles larger than 10 µm are difficult to transport without significant losses, therefore the actual measured size range is closer to 1–10 µm than the nominal 0.5–20 µm. Averaging time for the APS measurements was one minute. We note that none of the size distribution instruments could measure efficiently in the range of 0.5–1 µm, which certainly contained substantial amount of submicrometer mass concentration.

In this study, the SMPS was used to determine the mass concentration of particles with aerodynamic diameter below 0.5 µm ($PM_{0.5}$), which is used as a proxy for fine PM_1 particles. The mass concentration of particles with an aerodynamic diameter between 0.5 and 20 µm ($PM_{0.5–20}$) were measured with the APS, and this is used as a proxy for coarse supermicrometer PM_{10} particles. The mass concentrations of particles on the basis of the SMPS measurements were calculated based on the ToF-ACSM measurement results indicating that $PM_{0.5}$ consisted mainly of organics and BC and thus the estimated average particle density based on the chemical composition was 1.4 kg m^{-3}. $PM_{0.5–20}$ measured with the APS was assumed to consist mainly of mineral dust and thus particle density of 2.0 kg m^{-3} was used in the calculations.

Filter and impactor measurements

Particulate matter samples were collected to the filter substrate for in-depth chemical characterization. Two different filter sampling methods were used. In the first one, ambient air (11 LPM) was drawn through a filter (47-mm PTFE membrane filter, 3 µm pore size, Millipore, US) which separated particles from the sample air. At the air intake (inlet) supermicrometer (D_p > 1 µm) particles were removed using a cyclone (BGI 1.829, BGI, Inc., Waltham, MA, US). As a result, particles with aerodynamic diameter smaller than 1 µm were collected on the filter (called hereafter PM_1 filter collection). In addition, PM samples were collected to the PTFE filters for size-segregated chemical characterization (air flow 10 LPM) with a multistage impactor Nano Micro–Orifice Uniform Deposit Impactor (Nano-MOUDI, Model 125R, MSP Co., Marple *et al.*, 1991). The Nano-MOUDI divides particles based on their aerodynamic diameter into 13 different size classes between 10 nm and 10 µm. Collection times for both methods were 24 hours during weekdays and 72 hours during weekends. Altogether 13 PM_1 filter and Nano-MOUDI collections were made during the intensive campaign.

The gravimetric mass from the PM_1 PTFE filter samples was measured with an ultra-microbalance (UMT2, Mettler Toledo, US) in a humidity controlled chamber (RH 50% ± 5%). The major inorganic ions (Na^+, NH_4^+, K^+, Cl^-, NO_3^-, SO_4^{2-}) were analysed from the filter and impactor samples with the DX-2000 ion chromatographs (IC, Dionex, Sunnyvale, US). The ion chromatographic analysis method is described in detail by Timonen *et al.* (2014). The elemental composition (Al, As, Ba, Ca, Cd, Co, Cr, Cu, Fe, K, Mg, Mn, Na, Ni, Pb, V, Zn, Ba) from the PM_1 filters was determined using the inductively coupled plasma mass spectrometry (ICP–MS, DRC II, Perkin-Elmer SCIEX, Canada) and inductively coupled plasma optical emission spectrometry (ICP–OES, Vista Pro Radial, Varian Inc., Australia). The Energy Dispersive X-ray Fluorescence (EDXRF, Epsilon 5, PANalytical, Netherlands) was used to analyse the elemental composition (Al, As, Br, Ca, Cd, Cl, Cu, Cr, Fe , K, Mg, Mn, Mo, Ni, P, Pb, Rb, S, Sb, Se, Si, Sr, Ti, V, Zn, Zr) of the Nano-MOUDI samples. Impactor data was further analysed using data inversion (Wolfenbarger and Seinfeld, 1990) and mode fitting (Winklmayr *et al.* 1990) procedures.

Back trajectory modelling

Three day air mass backward trajectories were calculated to establish the origins and transport history of clean arctic air mass and the long-range transport (LRT) event. The trajectories

were calculated using the NOAA Hybrid Single-Particle Lagrangian Integrated Trajectory model (Stein *et al.* 2015, Rolph *et al.* 2017) and global meteorological data from the Global Data Assimilation System (GDAS) archive. The GDAS data has a 3-h time resolution, horizontal resolution of 1° × 1° and a vertical resolution of 23 pressure surfaces between 1000 and 20 hPa.

Results

PM mass concentrations, composition and size distribution

The measurement point of this study was situated next to the road leading to the mine pit. The distance of the measurement container from the edge of the mine pit was only ~150 m, suggesting that the measurements were strongly influenced by the traffic to the mine pit and PM produced by mining activities. During the measurement campaign ambient sub- and supermicrometer PM mass concentrations were on average 2.80 and 11.2 µg m^{-3}, respectively, and on average 80% of measured PM mass was attributed to supermicrometer particles. However, a large variation in both submicrometer (hourly average concentrations up to 18 µg^{-3}) and supermicrometer (hourly average concentrations up to 200 µg m^{-3}) size fractions were detected during the measurement period (Fig. 1c). Most typically the submicron PM was dominated by black carbon and organic fraction, however, occasional increases in sulphate concentrations were also observed (Fig. 1a and b). The variation is discussed more closely in the next paragraphs.

The sub- and supermicron PM concentrations were observed to be strongly dependent on the wind direction (Fig. 2), as can be expected for the measurements next to the PM source. When the wind was in the sector 70°–230°, it transported particles from the mine pit and passing vehicles related to mining to the measurement site. When the wind brought PM from the mining area, elevated submicron PM and supermicrometer PM concentrations (hourly average concentrations up to 18 and 200 µg m^{-3}) were observed, respectively. The measured number and mass size distributions show that simultaneously with the increase in coarse particle mass, elevated concentrations of submicrometer particles were observed (Figs. 1, 3 and 4). The largest number concentrations were observed for particles with the mobility diameter D_p < 100 nm.The mass size distributions of submicron PM show that the highest PM mass concentrations were observed for the particles at sizes between 100 and 500 nm (Fig. 4). These accumulation mode particles can be originating either from a local source (i.e. vehicles or mining activities) or they can be regional or long-range transported (Timonen *et al.* 2008, Niemi *et al.* 2009) aerosol. The areas north from the Kevitsa mine are mainly uninhabited and lacking any major anthropogenic PM sources. However, industrial activities e.g. smelters located in Koala Peninsula, northeast from Kevitsa, have been previously seen to influence air quality in northern Finland (Brus *et al.* 2013, Kyrö *et al.* 2014).

In order to further characterize the submicron particulate matter, elemental and ionic composition of PM collected on the PM_1 filters was analysed. The major water-soluble inorganic ions observed in the PM_1 filter samples were sulphate and ammonium but occasionally the concentrations of Mg^{2+}, Ca^{2+}, Na^+ and Cl^- were slightly elevated (Fig. 5). Similar inorganic ion concentrations and contributions are typically observed in Finland in urban and urban background sites (e.g. Timonen *et al.* 2014, Aurela *et al.* 2015), suggesting that there are no major sources of inorganic ions in the vicinity of the mine area. Only exception of the composition was observed for the sample collected at 12–13 May 2014. During that low PM concentration episode elevated sulphate concentrations (24-h average 2 µg m^{-3}) were observed. This episode is further discussed at chapter "Composition of PM in arctic air mass". In elemental analysis the highest concentrations were observed for the elements closely related to the crustal composition: Al, Fe, Ca, Na, K and Mg (Fig. 5). In addition, elevated concentrations were observed for Cr, Cu, Mn, Ni, V and Zn (Fig. 5).

Sulphate concentration in submicron particles was analyzed online with the ToF-ACSM and from the PM_1 filters in the laboratory. A good correlation between the methods was generally observed (Fig. A1) suggesting that both

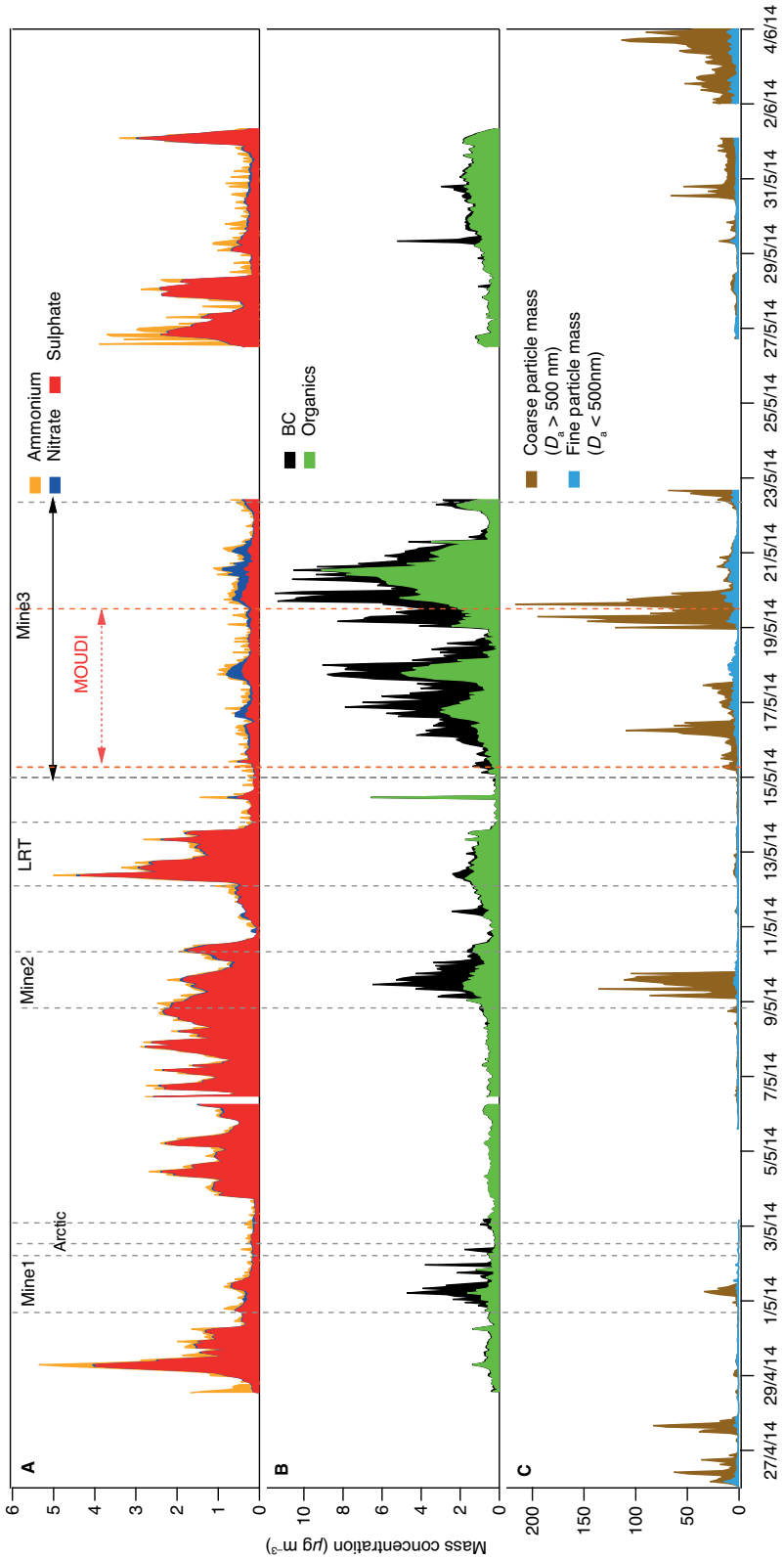

Fig. 1. Chemical composition of submicron PM and mass concentrations. (**A**) inorganic ion concentrations (ToF-ACSM), (**B**) Organics (ToF-ACMS) and BC (MAAP), (**C**) submicron PM concentration (aerodynamic diameter D_a < 500 nm, SMPS) and supermicron PM (D_a between 0.5–20 μm, APS)) during the measurement period (25 April–4 June 2014). Episodes and the analyzed MOUDI collection marked to the figure with dash lines.

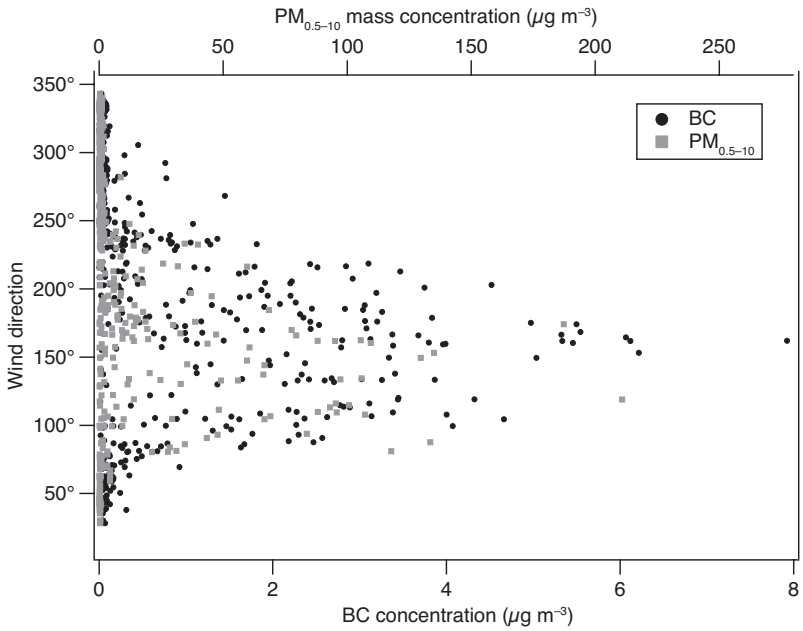

Fig. 2. Observed $PM_{0.5–10}$ mass concentrations and sub-micrometer black carbon concentrations as a function of wind direction. Highest concentrations for both fine and coarse particles were observed when the wind was blowing from the mine pit sector between 80°–220°.

methods are suitable for the measurements in the mining environment. However, online instrument enables the observation of rapid changes in PM concentrations, PM diurnal variations and comparison of the data with other continuously measured data such as the meteorological data.

PM chemical composition of PM originating from different sources

The observed submicron PM concentrations in the proximity of the open pit mine were typically low (< 5 μg m^{-3}, Fig. 1), but there were four distinct events with elevated concentrations of submicrometer and/or supermicrometer PM, which were selected for further investigation. The episode times, PM concentrations for different size fractions and main chemical species are given in Table 1. Very different chemical composition and size distributions for PM were observed during these episodes (Figs. 6 and 7). Three of these events had high sub- and supermicrometer PM concentrations. Local wind direction measurements indicate that wind brought air and mining emissions from the mine pit to the measurement site. These episodes were interpreted to originate from mining activities and are called hereafter Mine 1–3 episodes. During the fourth event, back trajectories indicate that air mass was brought to the measurement site from north Siberia via Koala Peninsula. This episode is called LRT episode. In addition to aforementioned episodes, a reference period was chosen to represent a situation when wind brought clean arctic air to the measurement site. This is called Arctic episode. In the following chapters there is a detailed description of each event.

Size resolved composition of PM originating from mining activities

Composition and sources of submicron PM produced by mining activities

During Mine 1–3 events, elevated concentrations of submicron particles, 5–18 μg m^{-3}, and supermicrometer particles, 40–200 μg m^{-3}, were observed (Figs. 1 and 5). Composition measurements with the ToF-ACSM and MAAP show that during these episodes PM_1 particles consisted mainly of organic compounds (31%–46%) and black carbon (44%–48%) (Fig. 6). Similar chemical composition with dominating carbonaceous fraction have been typically found in the exhaust particles of diesel engine powered vehicles (e.g. Karjalainen *et al.* 2015). The organic to

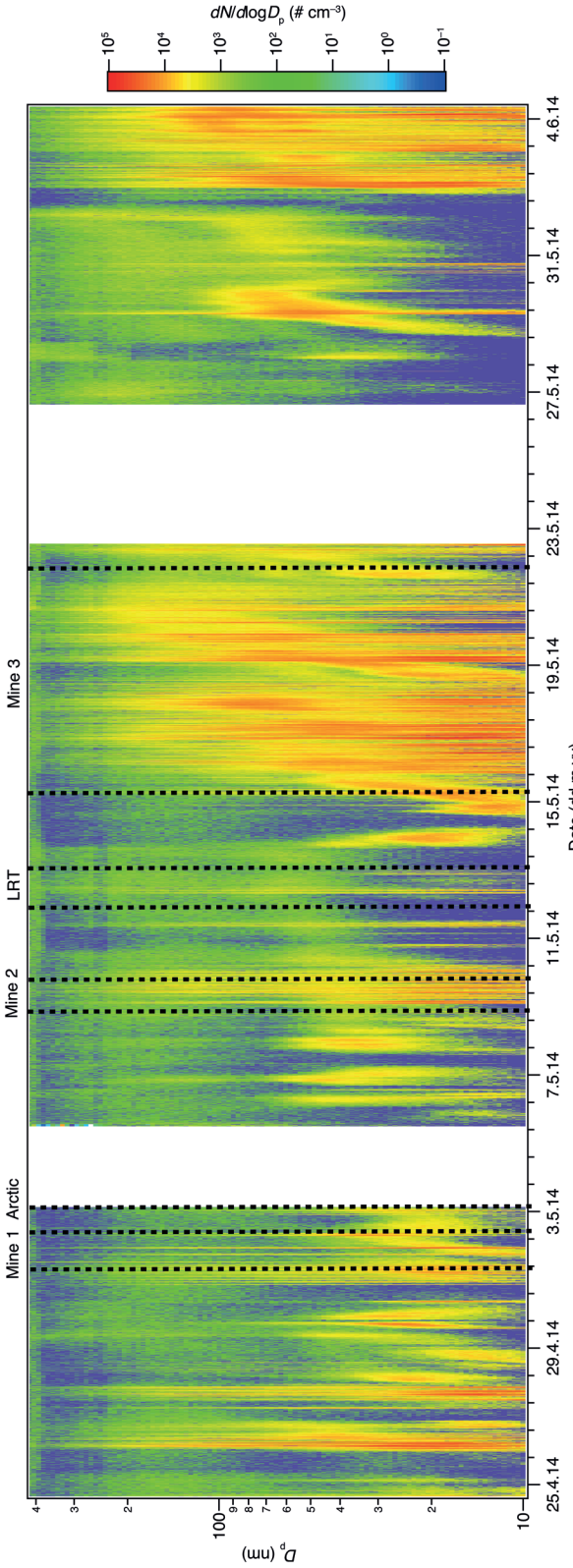

Fig. 3. Particle number concentration (SMPS, Aerodynamic diameter $D_a < 500$ nm) during the measurement period.

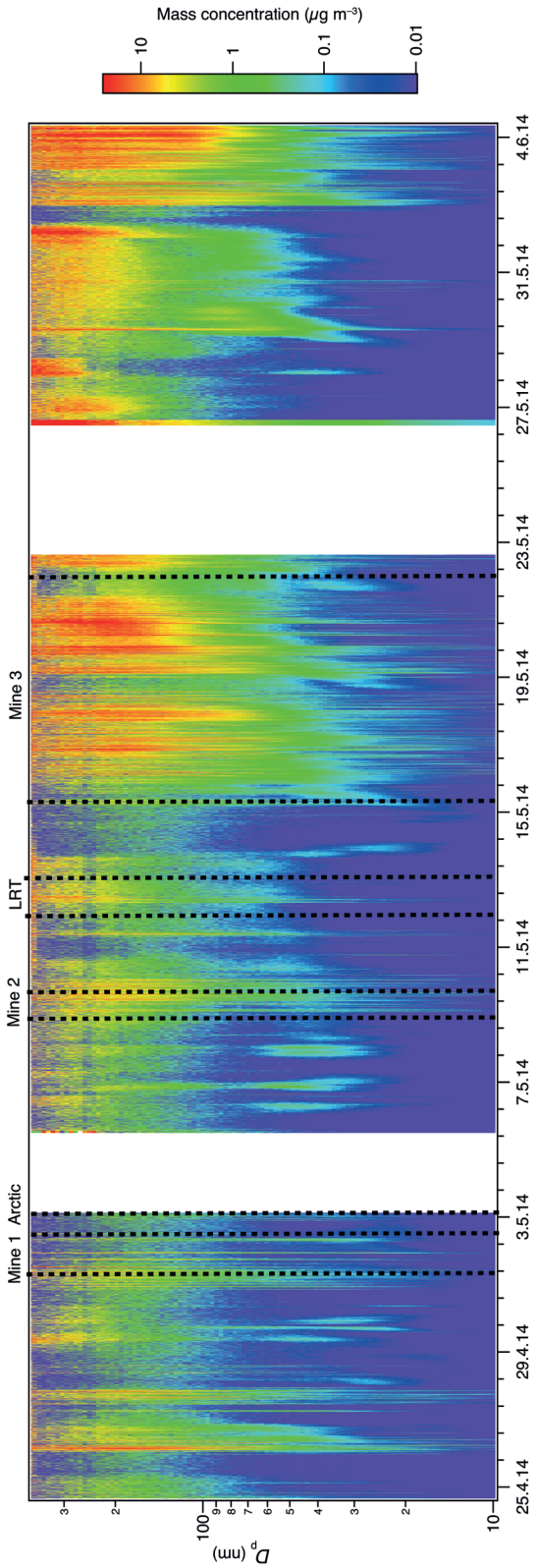

Fig. 4. Mass concentration of particles (SMPS, Aerodynamic diameter $D_a < 500$ nm) during the measurement campaign (25 April–4 June 2014).

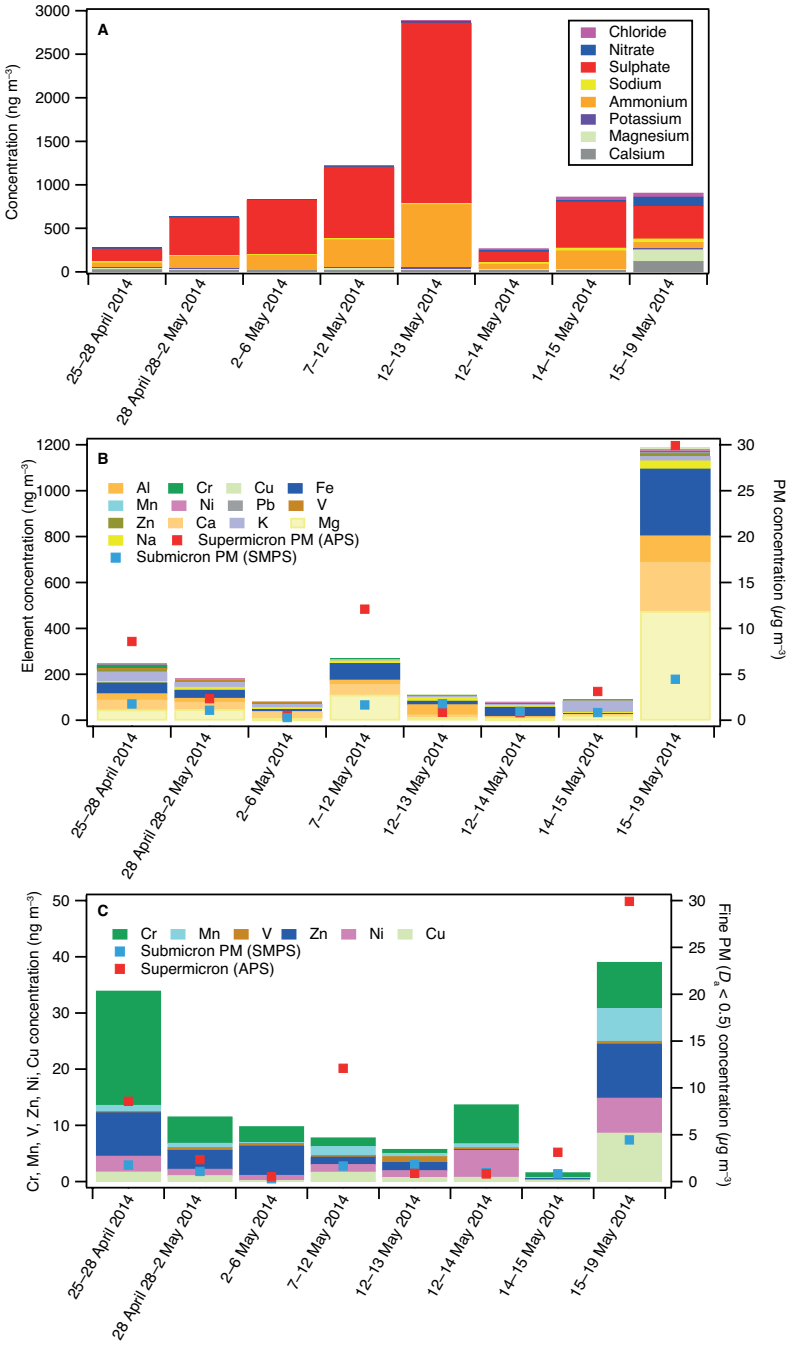

Fig. 5. Concentrations of (**A**) inorganic ions, (**B**) all analyzed elements and (**C**) Cr, Cu, Mn, Ni, V and Zn analyzed from the PM_1 filters. Submicron (SMPS) and supermicron PM (APS) concentrations marked with blue and red squares in **B** and **C**.

elemental carbon (OC/EC) ratios were between 0.65 and 1. Low OC/EC-ratios are typically associated with freshly emitted PM (Aurela *et al.* 2011). During these episodes contribution of inorganic ions in PM was low. Also, the highest number concentrations (Fig. 3) were observed for the particles with diameter smaller than 100 nm. Vehicles exhaust emissions are known to contain large concentrations of small nanoparticles (e.g. Rönkkö *et al.* 2014, 2017, Pirjola *et al.* 2015). Based on composition, chemical characteristics and size distribution, the most likely

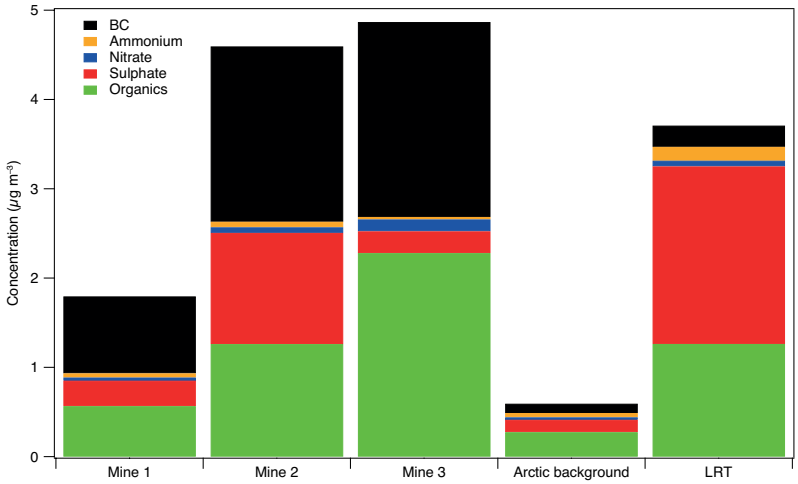

Fig. 6. PM_1 composition during the chosen periods representing emissions from mining activities (Mine 1–3), arctic background air and LRT emissions (LRT).

source of PM_1 particles was vehicular activities in the mine area. This is further supported by the elemental analysis of PM_1 samples, where elevated concentrations of V and Zn, which are typically originated from traffic emissions, were observed (Fig. 5). Additionally, in elemental analysis, high metal concentrations for several elements Mg, Ca, Al, Fe, that are typically observed in earth crust, was observed for the PM_1 sample collected during Mine 3 episode (15–19 May 2014) indicating that mineral dust can be seen also in submicron particles.

Composition and sources of supermicron PM produced by mining activities

During the Mine events, the largest increase was seen for supermicrometer particles, likely due to mineral dust from mining activities e.g. ore loading and hauling, and resuspension of dust from dry ground surface. In order to study the size distributions of PM originating from mining activities, eight size resolved PM samples with the Nano-MOUDI were collected during the measurement campaign. However, due to poor time resolution (up to 72 h), most samples were the mixtures of PM originating from several sources and therefore were not considered to be representative of mining emissions. One of the samples was collected during Mine 3 episode (15–19 May 2014 first half of episode 3) and was therefore chosen for in-depth analysis using the XRF in order to study the size distribution of elements originating from mining activities. Results show that this sample had high PM loadings (constructed by summing up all the elements found by the XRF analysis) and the supermicrometer particles were dominating the mass size distribution (Fig. 8). In the size distri-

Table 1. Observed episodes and average PM_1 (sum of BC, ions, Organic matter), BC (MAAP), inorganic ion (sum of sulphate, ammonium, nitrate from ToF-ACSM) and organic matter (ToF-ACSM) concentrations during the episodes.

Episode	Time	BC (μg m^{-3})	Inorganic ions (μg m^{-3})	Organic matter (μg m^{-3})	PM_1 (ToF-ACSM) (μg m^{-3})	$PM_{0.5}$ (SMPS) (μg m^{-3})	$PM_{0.5–20}$ (APS) (μg m^{-3})
Mine 1	31 April, 23:00 to 2 May , 08:00	0.9	0.4	0.6	1.8	1.3	8.7
Mine 2	9 May, 02:00 to 10 May, 03:00	2.0	1.4	1.3	4.6	3.0	62.9
Mine 3	15 May, 06:00 to 21 May, 12:00	2.2	0.4	2.3	4.9	5.4	26.6
Arctic	2 May , 10:00 to 3 May, 03:00	0.1	0.2	0.3	0.6	0.4	*
LRT	12 May , 05:00 to 13 May , 11:00	0.2	2.2	1.3	3.7	2.0	0.9

* no APS data available.

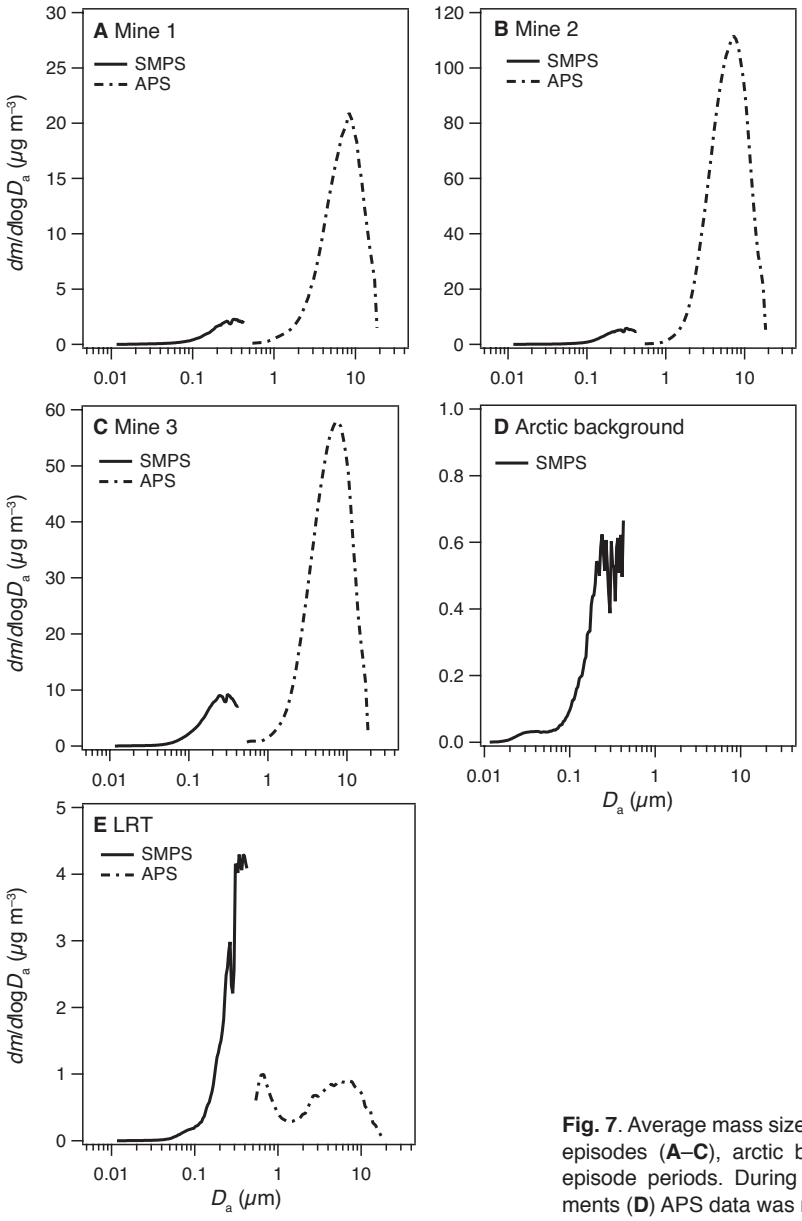

Fig. 7. Average mass size distributions for the Mine 1–3 episodes (**A**–**C**), arctic background (**D**) and LRT (**E**) episode periods. During Arctic background measurements (**D**) APS data was not available.

butions of individual elements four modes with the mass median diameters 0.15, 0.50. 2.1 and 6.5 µm were typically found (Figs. 8 and A2). For most elements, the largest mode in size was dominating. However, for sulphur, submicron modes were dominating and it had similar size distribution in submicron modes as ammonium. Similar sulphate size distributions with dominating accumulation mode have been observed in the ambient studies for long-range transported aerosols (e.g. Timonen *et al.* 2008). The minor supermicrometer mode of sulphate correlated with the modes of crustal elements.

One way to analyse elemental composition, and the contribution of mineral dust on it, is to compare achieved concentrations to average crustal composition (Mason 1966). Enrichment from the average crustal composition can be calculated using the following equation:

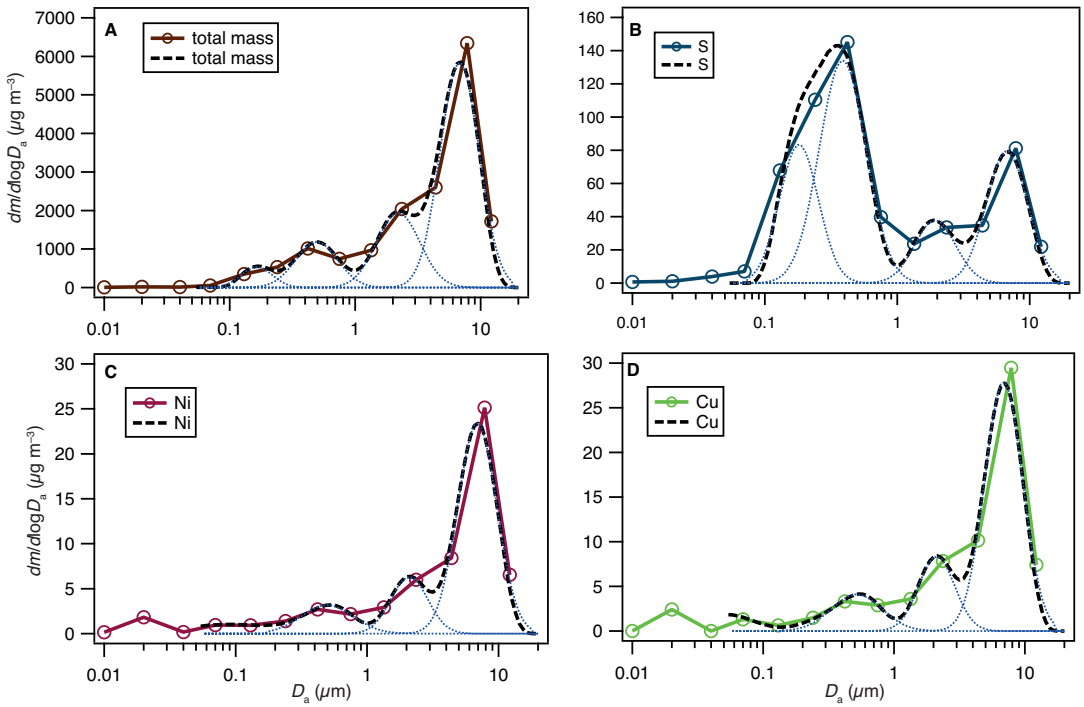

Fig. 8. (**A**) Average mass (sum of elements found in the XRF analysis), (**B**) sulphur, (**C**) nickel and (**D**) copper size distributions in the Nano-MOUDI collection over 15–19 May 2014 shows that coarse particles from resuspension caused by vehicles and from other mining activities dominate the mass concentration during the episodes. Raw data (data points), inverted (dashed line) and found individual particle modes are shown.

$$\text{Enrichment factor}\left(\text{EF}\right)=\frac{\left(\text{Element}_i/\text{Element}_{\text{ref}}\right)_{\text{measured}}}{\left(\text{Element}_i/\text{Element}_{\text{ref}}\right)_{\text{crustal average}}},\ (1)$$

where Element_i is the element which is studied and $\text{Element}_{\text{ref}}$ is the element used as a reference. Here Si was selected as a reference element. The crustal average is taken from literature (Mason 1966). Results are shown in Table 2 separately for different particle size modes (size distributions shown in Figs. 8 and A2). The method is rough and therefore only values significantly different from one can be predicted to be an indication of enrichment from universal crustal average. In the studied Nano-MOUDI sample, only Mg, S, Ni and Cu are clearly enriched. Enrichment of Ni and Cu is in line with the fact that probably resuspended dust includes material from ores. Nickel in Kevitsa is in the form of nickel sulphate, which could be one source of observed sulphur concentrations in submicron particles. For all the other elements composition corresponds roughly crustal average. The contribution of mineral dust in coarse particles is overwhelming and based on enrichment factors dust has also a significant fine particle fraction (Table 2). However, in an impactor sampling there is always a risk that for high loadings particles bounce and are not collected by the

Table 2. Enrichment of elements for four size distribution modes (with mass median diameters approximately 0.15, 0.50. 2.1 and 6.5 μm) observed in the Nano-MOUDI collection (15–19 May 2014).

Element	Mode 1	Mode 2	Mode 3	Mode 4
Al	0.40	0.40	0.43	0.44
Ca	2.90	3.06	2.96	3.71
Ti	–	1.66	1.05	2.49
Fe	2.67	2.55	2.43	3.79
Mn	3.24	3.00	2.37	3.18
Na	0.52	1.25	1.12	0.24
Mg	7.00	11.35	6.25	6.45
S	961	1036	653	745
Ni	–	41.24	30.63	42.04
Cu	–	70.65	54.35	66.63

desired stage, and continue to lower stages. Therefore it cannot be ruled out that a part of the mass found in the sub-micrometer stages is due to bounce-off of larger particles from the upper stages. The mass size distributions measured with the Nano-MOUDI (Figs. 8 and A2) and the on-line mass size distribution measurements (SMPS and APS) averaged over the sampling times of the Nano-MOUDI (Fig. 7, episode 3) were very similar. However, the mode at 2 µm in the Nano-MOUDI distribution was not seen in the mass size distribution measured on-line (Fig. 7), which might be an indication of particle bounce-off from the upper stages and collection by the stages around 2 µm.

Six components were analysed both as an element (Na, Cl, Ca, K, S and Mg) and an ion (Na^+, Cl^-, Ca^{2+}, K^+, SO_4^{2-} and Mg^{2+}) form from Mine 3 sample (15–19 May 2014) using EDXRF and ion chromatography, respectively. The size distributions for Na, Cl, Ca, K and S were similar for both analytical methods indicating that the elements were mainly in water-soluble ions (Fig. A3a). Mg is an exception as most of it seemed to be insoluble and not in the form of soluble compound containing Mg^{2+}-ion. Similar size distribution with dominating submicron modes was observed for sulphur for both analytical methods suggesting that sulphur in the submicron modes was dominated by sulphate, which is formed in the atmosphere from SO_2 precursor via oxidation. If ammonia is available, sulphate is in the form of diammonium sulphate (fully neutralized by ammonia) or ammonium bisulphate. Figure A4b presents the size distributions of sulphate, ammonium and nitrate. Below 1 µm sulphate was clearly in the form of diammonium sulphate confirmed by an ion equivalent ratio (Fig. A4). For pure ammonium bisulphate or diammonium sulphate the ratios are 1 and 0.5, respectively. In particles with aerodynamic diameter $D_a > 1$ µm, ammonium concentration was low and therefore supermicrometer sulphate was most likely as a salt of alkaline metal from mineral dust (e.g. $CaSO_4$) (Fig. A2). Nitrate was mainly found in coarse particles and probably follows from the reaction of nitric acid with sea salt (sodium chloride) during transport from more polluted areas to the region. Local NO_2 emissions from diesel engines do not necessarily contribute to observed coarse particle nitrate because of too short residence time for NO_2 to nitric acid conversion.

Composition of PM during the LRT episode

The air mass back trajectories indicate that during the fourth event (12–13 May 2014) the air mass was long-range transported from north Siberia over Kola Peninsula, where metallurgical industry is operated (Fig. A5). Smelter industry is known to produce high SO_2 emissions, and elevated sulphate concentrations have been occasionally also observed in northern Finland (Brus *et al.* 2013, Kyrö *et al.* 2014). This event is called LRT episode. During the LRT episode high sulphate concentrations (up to 5 µg m^{-3}) in submicron particles were observed (Fig. 1). However, BC and supermicrometer particle mass concentrations were very low. The contribution of sulphate to PM mass was 54%, whereas the contributions of organics and BC were 34% and 6% (Fig. 6). The OC/BC ratio was much higher (5.3) than for the mining emissions. Elevated OC/EC ratios were also observed for LRT aerosols in previous studies (e.g. Timonen *et al.* 2014, Aurela *et al.* 2011), likely due to the secondary organic aerosol formation increasing OC during transport.

Composition of PM in arctic air mass

In addition to aforementioned episodes, a reference period (called arctic episode hereafter) was chosen to represent the situation when wind brought clean arctic air with low PM (below 3 µg m^{-3}) to the measurement site. During the arctic episode period PM_1 concentration was on average 2 µg m^{-3} (Figs. 1, 3 and 4). Inorganic species (75%) and organic compounds (24%) dominated PM_1 mass, whereas black carbon concentration was very low (contribution approximately 1%) (Figs. 1 and 6). During the reference period the composition was similar to the composition typically observed for clean arctic air masses (e.g. Timonen *et al.* 2014). The size distribution was dominated by the accumulation mode particles. However, due to the malfunction of the APS coarse particle concentration is not available for this episode.

Comparison to ambient PM levels

In order to assess the PM levels measured next to the Kevitsa mine, PM concentrations at the open pit mine area were compared with average ambient $PM_{2.5}$ and PM_{10} levels for typical urban and rural areas in Finland (Laakso *et al.* 2003) as well as the PM levels measured in an underground mine (Saarikoski *et al*. 2017). For more detailed comparison, Kevitsa data was split into episodic (Mine 1–3) and non-episodic PM concentrations. The non-episodic and episodic submicron PM (SMPS $PM_{0.5}$ used as a proxy) concentrations at Kevitsa measured during the measurement period are on the same level as typically observed in rural background areas (Fig. 9). Episodic submicron PM values represent the situation when wind brought air directly from the mine pit to the measurement site. Even during these episodes the observed submicron PM concentrations were significantly lower than PM concentrations observed in the underground mine (Saarikoski *et al*. 2017). PM_{10} concentrations during the episodes were significantly higher than urban or even rural PM_{10} concentrations but were on the same level with the underground mine.

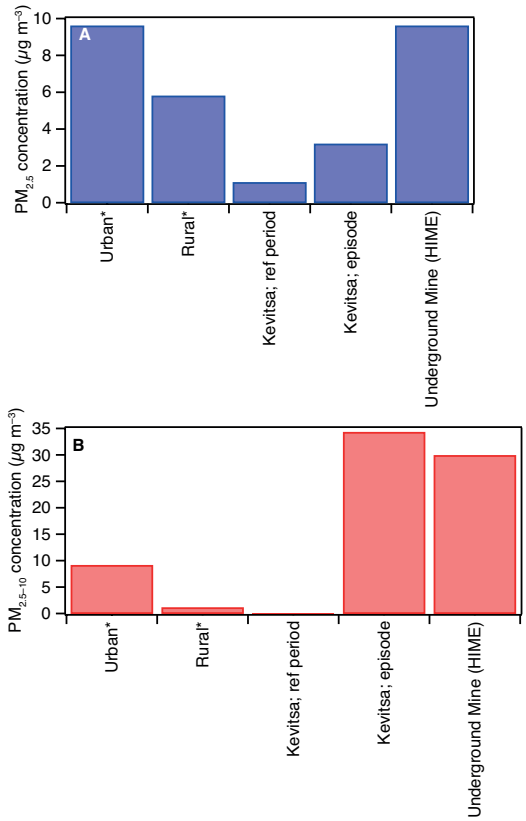

Fig. 9. (**A**) Submicron and (**B**) supermicron PM concentrations observed in the Kevitsa mine compared to the ambient PM concentrations in urban and rural areas (Laakso *et al.* 2003). $PM_{2.5–10}$ calculated by subtracting $PM_{2.5}$ from PM_{10}) as well as average PM concentrations observed in an underground mine. Reference period and episode times are given in Table 1. Values given for episodic periods are average values for all episodes.

Conclusions

Mining activities are known to produce particulate matter emissions. From open pit mining, particles (e.g. mineral dust, vehicular engine emissions) are quickly diluted to surrounding air and the transport via air to the nearby environment is quite unrestricted. Detailed information about chemical and physical characteristics of particles in the vicinity of actively operating mining environments is scarce. This study investigated the composition and concentrations of PM emitted from mining activities next to the open pit mine in Finnish Lapland. PM next to the open pit mine consisted mainly of supermicrometer particles (80%) and only a smaller fraction (20%) was attributed to submicron particles, on average. Elevated PM concentrations were observed only during the periods when wind blew directly from the mine pit. During these periods observed PM concentrations were relatively high, especially for supermicrometer particles (up to 200 μg m^{-3}). However, the measured PM_{10} emissions are lower or in similar level than typical urban road dust emissions observed from paved roads (e.g. Pirjola *et al.* 2010). Also, since the lifetime of supermicrometer particles in the atmosphere is very limited, the influence of PM from mining activities on surrounding nature and on people living near mines is likely relatively small and very local.

Submicron particles contained mainly BC and organic matter, and were strongly associated with vehicular emissions in the mining environment. BC absorbs solar radiation and

thus promotes climate change. Furthermore BC could have adverse influences in snow covered arctic areas due to decrease in the surface albedo. However, due to the dilution the concentrations were fairly low (< 2.2 µg m^{-3}) even next to the mine. Additionally, detailed composition analysis indicated that in addition to vehicular emissions long-range transport of submicron PM from Koala peninsula or northern Siberia and also mineral dust were increasing submicron PM levels occasionally. The composition and size distribution of PM originating from the mining emissions were very different compared with clean arctic air PM and LRT episodes. To put observed submicron PM concentrations in perspective, average submicron mass concentrations (2.80 µg m^{-3}) measured next to the actively operating open pit mine were on the same level with the concentration measured in rural areas. In Finland, the mining is concentrated to northern Finland with low population density and therefore the exposure of local inhabitants to the mining emissions is likely low.

This study showed that advanced aerosol measurement technology was well suited the generally harsh environmental conditions of the mines and arctic areas. The information achieved is unique, because this is the first time when real-time, detailed and source-specific information on particle chemical composition next to the open pit mine became available. The achieved results reveal the major sources of particulate matter in mine and helps in arranging better control systems and health risk assessments. Additionally, the data can be useful for modeling the influences of particulate matter released by a mine on air quality, human health and climate in the future.

Acknowledgements: The staff of Boliden Kevitsa mine is gratefully acknowledged for their invaluable help during the measurement campaign. This research was funded by TEKES Green Mining program (HIME project) and Academy of Finland (MISU program/PARMAT project 297804). Support from Mike Cubison during the campaign and in data handling is gratefully acknowledged. The authors gratefully acknowledge the NOAA Air Resources Laboratory (ARL) for the provision of the HYSPLIT transport and dispersion model and/or READY website (http://www.ready.noaa.gov) used in this publication

References

Aneja V.P., Isherwood A. & Morgan P. 2012. Characterization of particulate matter (PM_{10}) related to surface coal mining operations in Appalachia. *Atmos. Environ.* 54: 496–501.

Bradley R.S., Vuille M., Diaz H.F. & Vergara W. 2006. Climate change. Threats to water supplies in the tropical Andes. *Science* 312: 1755–1756.

Brus D., Neitola K., Asmi E., Aurela M., Makkonen U., Svensson J., Hyvärinen A.P., Hirsikkoa A., Hakola H., Hillamo R. & Lihavainen H. 2013. Pallas cloud experiment, PaCE 2012. *AIP Conf. Proc.* 1527: 964–967.

Canagaratna M.R., Onasch T.B., Wood E.C., Herndon S.C., Jayne J.T., Cross E.S., Miake-Lye R.C., Kolb C.E. & Worsnop D.R. 2010. Evolution of Vehicle Exhaust Particles in the Atmosphere. *J. Air & Waste Manage. Assoc.* 60: 1192–1203.

Csavina J., Landazuri A., Wonaschutz A., Rine K., Rheinheimer P., Barbaris B., Conant W., Saez A.E. & Betterton E.A. 2011. Metal and Metalloid Contaminants in Atmospheric Aerosols from Mining Operations. *Water Air Soil Pollut.* 221: 145–157.

Flanner M.G., Zender C.S., Randerson J.T. & Rasch P.J. 2007. Present-day climate forcing and response from black carbon in snow. *J. Geophys. Res*. 112, doi:10.1029/2006jd008003.

Fröhlich R., Cubison M.J., Slowik J.G., Bukowiecki N., Prévôt A.S.H., Baltensperger U., Schneider J., Kimmel J.R., Gonin M., Rohner U., Worsnop D.R. & Jayne J.T. 2013. The ToF-ACSM: a portable aerosol chemical speciation monitor with TOFMS detection. *Atmos. Meas. Tech.* 6: 3225–3241.

Ghose M.K. 2007. Generation and Quantification of Hazardous Dusts from Coal Mining in the Indian Context. *Environ. Monit. Assess* 130: 35–45.

Gonzales P., Felix O., Alexander C., Lutz E., Ela W. & Sáez A.E. 2014. Laboratory dust generation and size-dependent characterization of metal and metalloid-contaminated mine tailings deposits. *J. Hazard. Mater.* 280: 619–625.

Hienola A.I., O'Donnell D., Pietikäinen J.-P., Svensson J., Lihavainen H., Virkkula A., Korhonen H. & Laaksonen A. 2017. The radiative impact of Nordic anthropogenic black carbon. *Tellus* 68B: 27428, doi:10.3402/tellusb.v68.27428.

IARC 2012. International Agency for Research on Cancer (IARC) of WHO, Press release no. 213, 2012.

Järvi L., Hannuniemi H., Hussein T., Junninen H., Aalto P.P., Hillamo R., Mäkelä T., Keronen P., Siivola E., Vesala T. & Kulmala M. 2009. The urban measurement station SMEAR III: Continuous monitoring of air pollution and surface-atmosphere interactions in Helsinki, Finland. *Boreal Env. Res.* 14: 86–109.

Karjalainen P., Timonen H., Saukko E., Kuuluvainen H., Saarikoski S., Aakko-Saksa P., Murtonen T., Bloss M., Dal Maso M., Simonen P., Ahlberg E., Svenningsson B., Brune W.H., Hillamo R., Keskinen J. & Rönkkö T. 2016. Time-resolved characterization of primary parti-

cle emissions and secondary particle formation from a modern gasoline passenger car. *Atmos. Chem. Phys.* 16: 8559–8570.

Khan A.L., Dierssen H., Schwarz J.P., Schmitt C., Chlus A., Hermanson M., Painter T.H. & McKnight D.M. 2017. Impacts of coal dust from an active mine on the spectral reflectance of Arctic surface snow in Svalbard, Norway. *J. Geophys. Res.* 122: 1767–1778.

Kyrö E.-M., Väänänen R., Kerminen V.-M., Virkkula A., Petäjä T., Asmi A., Dal Maso M., Nieminen T., Juhola S., Shcherbinin A., Riipinen I., Lehtipalo K., Keronen P., Aalto P.P., Hari P. & Kulmala M. 2014. Trends in new particle formation in eastern Lapland, Finland: effect of decreasing sulfur emissions from Kola Peninsula. *Atmos. Chem. Phys.* 14: 4383–4396.

Laakso L., Hussein T., Aarnio P., Komppula M., Hiltunen V., Viisanen Y. & Kulmala M. 2003. Diurnal and annual characteristics of particle mass and number concentrations in urban, rural and Arctic environments in Finland. *Atmos. Environ.* 37: 2629–2641.

Lihavainen H., Hyvarinen A., Asmi E., Hatakka J. & Viisanen Y. 2015. Long-term variability of aerosol optical properties in northern Finland. *Boreal Env. Res.* 20: 526–541.

Maricq M. 2007. Chemical characterization of particulate emissions from diesel engines: A review. *J. Aerosol Sci.* 38: 1079–1118.

Marple V.A., Rubow K.L. & Behm S.M. 1991. A Microorifice Uniform Deposit Impactor (MOUDI): Description, Calibration, and Use. *Aerosol Sci. Tech.* 14: 434–446.

Mason B. 1966. *Principles of Geochemistry*. John Wiley, New York.

Meinander O., Kontu A., Virkkula A., Arola A., Backman L., Dagsson-Waldhauserová P., O. J., Manninen T., Svensson J., de Leeuw G. & Leppäranta M. 2014. Brief communication: Light-absorbing impurities can reduce the density of melting snow. *The Cryosphere* 8: 991–995.

Menon S., Koch D., Beig G., Sahu S., Fasullo J. & Orlikowski D. 2010. Black carbon aerosols and the third polar ice cap. *Atmos. Chem. Phys.* 10: 4559–4571.

Müller T., Henzing J.S., de Leeuw G., Wiedensohler A., Alastuey A., Angelov H., Bizjak M., Collaud Coen M., Engström J.E., Gruening C., Hillamo R., Hoffer A., Imre K., Ivanow P., Jennings G., Sun J.Y., Kalivitis N., Karlsson H., Komppula M., Laj P., Li S.M., Lunder C., Marinoni A., Martins dos Santos S., Moerman M., Nowak A., Ogren J.A., Petzold A., Pichon J.M., Rodriquez S., Sharma S., Sheridan P.J., Teinilä K., Tuch T., Viana M., Virkkula A., Weingartner E., Wilhelm R. & Wang Y.Q. 2011. Characterization and intercomparison of aerosol absorption photometers: result of two intercomparison workshops. *Atmos. Meas. Tech.* 4: 245–268.

Myung C.L., Ko A. & Park S. 2014. Review on characterization of nano-particle emissions and PM morphology from internal combustion engines: Part 1. *Int. J. Autom. Technol.* 15: 203–218.

Niemi J.V., Saarikoski S., Aurela M., Tervahattu H., Hillamo R., Westphal D.L., Aarnio P., Koskentalo T., Makkonen U., Vehkamäki H. & Kulmala M. 2009. Long-range transport episodes of fine particles in southern Finland during 1999–2007. *Atmos. Environ.* 43: 1255–1264.

Noll J.D., Bugarski A.D., Patts L.D., Mischler S.E. & McWilliams L. 2007. Relationship between elemental carbon, total carbon, and diesel particulate matter in several underground metal/non-metal mines. *Environ. Sci. Technol.* 41: 710–716.

Noll J.D., Mischler S.E., Patts L.D., Schnakenberg G.H., Bugarski A.D. & Timko R.J. 2006. The effects of water emulsified fuel on diesel particulate matter concentrations in underground mines. In: Mutmansky J.M. & Ramani R.V. (eds.), *Proceedings of the 11th U.S./North American Mine Ventilation Symposiums*, Taylor & Francis Group London, pp. 159–164.

Paatero P. 1997. Least squares formulation of robust non-negative factor analysis. *Chemometr. Intell. Lab.* 37: 23–35.

Paatero P. 1999. The multilinear engine – a table-driven, least squares program for solving multilinear problems, including the n-way parallel factor analysis model. *J. Comput. Graph. Stat.* 1: 854–888.

Pandey B., Agrawal M. & Singh S. 2014. Assessment of air pollution around coal mining area: Emphasizing on spatial distributions, seasonal variations and heavy metals, using cluster and principal component analysis. *Atmos. Pollut. Res*. 5: 79–86.

Peters T.M. & Leith D. 2003. Concentration measurement and counting efficiency of the aerodynamic particle sizer 3321. *J. Aerosol Sci.* 34: 627–634.

Petzold A. & Schönlinner M. 2004. Multi-angle absorption photometry — a new method for the measurement of aerosol light absorption and atmospheric black carbon. *J. Aerosol Sci.* 35: 421–441.

Pirjola L., Johansson C., Kupiainen K., Stojiljkovic A., Karlsson H. & Hussein T. 2010. Road Dust Emissions from Paved Roads Measured Using Different Mobile Systems. *J. Air & Waste Manage. Assoc.* 60: 1422–1433.

Pirjola L., Karl M., Rönkkö T. & Arnold F. 2015. Model studies of volatile diesel exhaust particle formation: Are organic vapours involved in nucleation and growth? *Atmos. Chem. Phys.* 15: 10435–10452.

Pope C.A., Dockery, D.W. 2006. Health Effects of Fine Particulate Air Pollution: Lines that Connect. *J. Air & Waste Manage. Assoc.* 56: 709–742.

Quinn P.K., Stohl A., Arneth A., Berntsen T., Burkhart J.F., Christensen J., Flanner M., Kupiainen K., Lihavainen H., Shepherd M., Shevchenko V., Skov H. & Vestreng V. 2011. *The Impact of Black Carbon on Arctic Climate*. AMAP Technical Report No. 4, Arctic Monitoring and Assessment Programme (AMAP), Oslo. Rolph G., Stein A. & Stunder B. 2017. Real-time Environmental Applications and Display sYstem: READY. *Environmental Modelling & Software* 95: 210–228.

Rönkkö T., Pirjola L., Ntziachristos L., Heikkilä J., Karjalainen P., Hillamo R. & Keskinen J. 2014. Vehicle engines produce exhaust nanoparticles even when not fueled. *Environ. Sci. Technol.* 48: 2043–2050.

Saarikoski S., Timonen H., Saarnio K., Aurela M., Järvi L., Keronen P., Kerminen V.M. & Hillamo R. 2008. Sources of organic carbon in fine particulate matter in northern European urban air. *Atmos. Chem. Phys.* 8: 6281–6295.

Saarikoski S., Teinilä K., Timonen H., Aurela M., Laaksovirta T., Reyes F., Vásques Y., Oyola P., Artaxo P., Pennanen A., Junttila S., Linnainmaa M., Salonen R., & Hillamo R. 2017. Particulate matter characteristics, dynamics and sources in an underground mine. *Aerosol Sci. Tech.* doi:10.1080/02786826.2017.1384788.

Schmale J., Flanner M., Kang S., Sprenger M., Zhang Q., Guo J., Li Y., Schwikowski M. & Farinotti D. 2017. Modulation of snow reflectance and snowmelt from Central Asian glaciers by anthropogenic black carbon. *Sci. Rep.* 7: 40501, doi:10.1038/srep40501.

Schwarz J.P., Gao R.S., Spackman J.R., Watts L.A., Thomson D.S., Fahey D.W., Ryerson T.B., Peischl J., Holloway J.S., Trainer M., Frost G.J., Baynard T., Lack D.A., de Gouw J.A., Warneke C. & Del Negro L.A. 2008. Measurement of the mixing state, mass, and optical size of individual black carbon particles in urban and biomass burning emissions. *Geophys. Res. Lett.* 35, doi:10.1029/2008gl033968.

Stein A.F., Draxler R.R., Rolph G.D., Stunder B.J.B., Cohen M.D. & Ngan F. 2015. Noaa's Hysplit Atmospheric Transport and Dispersion Modeling System. *Bull. Am. Meteorol. Soc.* 96: 2059–2077.

Tedesco M., Doherty S., Fettweis X., Alexander P., Jeyaratnam J. & Stroeve J. 2016. The darkening of the Greenland ice sheet: trends, drivers, and projections (1981–2100). *Cryosphere* 10: 477–496.

Thomas C.R. & Kelley T.R. 2010. A brief review of silicosis in the United States. *Environ. Health Insights* 4: 21–26.

Timonen H., Aurela M., Carbone S., Saarnio K., Frey A., Saarikoski S., Teinilä K. & Hillamo R. 2014. Seasonal and diurnal changes in inorganic ions, carbonaceous matter and mass in ambient aerosol particles in an urban, background area. *Boreal Env. Res.* 19: 71–86.

Timonen H., Carbone S., Aurela M., Saarnio K., Saarikoski S., Ng N.L., Canagaratna M.R., Kulmala M., Kerminen V.-M., Worsnop D.R. & Hillamo R. 2013. Characteristics, sources and water-solubility of ambient submicron organic aerosol in springtime in Helsinki, Finland. *J. Aerosol Sci.* 56: 61–77.

Timonen H., Cubison M., Aurela M., Brus D., Lihavainen H., Hillamo R., Canagaratna M., Nekat B., Weller R., Worsnop D. & Saarikoski S. 2016. Applications and limitations of constrained high-resolution peak fitting on low resolving power mass spectra from the ToF-ACSM. *Atmos. Meas. Tech.* 9: 3263–3281.

Timonen H.J., Saarikoski S.K., Aurela M.A., Saarnio K.M. & Hillamo R.E.J. 2008. Water-soluble organic carbon in urban aerosol: Concentrations, size distributions and contribution to particulate matter. *Boreal Env. Res.* 13: 335–346.

Ulbrich I.M., Canagaratna M.R., Zhang Q., Worsnop D.R. & Jimenez J.L. 2009. Interpretation of organic components from Positive Matrix Factorization of aerosol mass spectrometric data. *Atmos. Chem. Phys.* 9: 2891–2918.

Wang S.C. & Flagan R.C. 1990. Scanning Electrical Mobility Spectrometer. *Aerosol Sci. Tech.* 13: 230–240.

Winklmayr W., Wang H.C. & John W. 1990. Adaptation of the Twomey Algorithm to the Inversion of Cascade Impactor Data. *Aerosol Sci. Tech.* 13: 322–331.

Wolfenbarger J.K. & Seinfeld J.H. 1990. Inversion of Aerosol Size Distribution Data. *J. Aerosol Sci.* 21: 227–247.

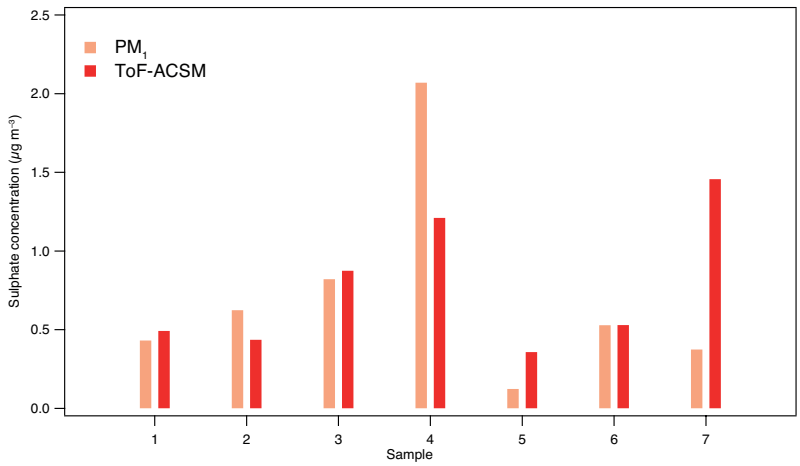

Fig. A1. Sulphate concentrations measured with ToF-ACSM and analyzed from PM_1 filters (samples 1–5) during the campaign.

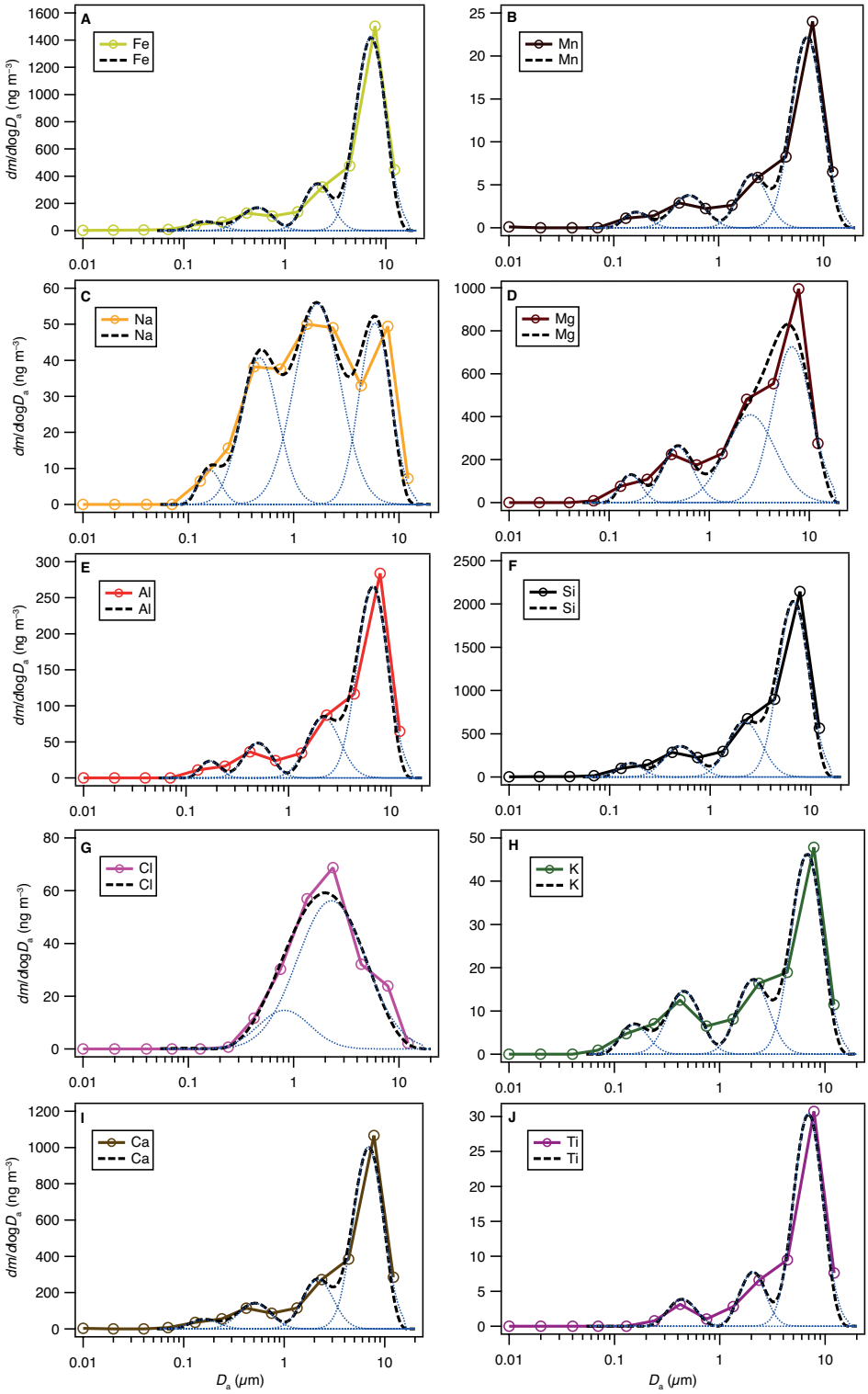

Fig. A2. Mass size distributions of elements found in the XRF analysis from the Nano-MOUDI collection (15–19 May) shows that the highest mass concentrations of crustal elements are in super-micrometer particles. Submicrometer sulphur was mainly long-range transported.

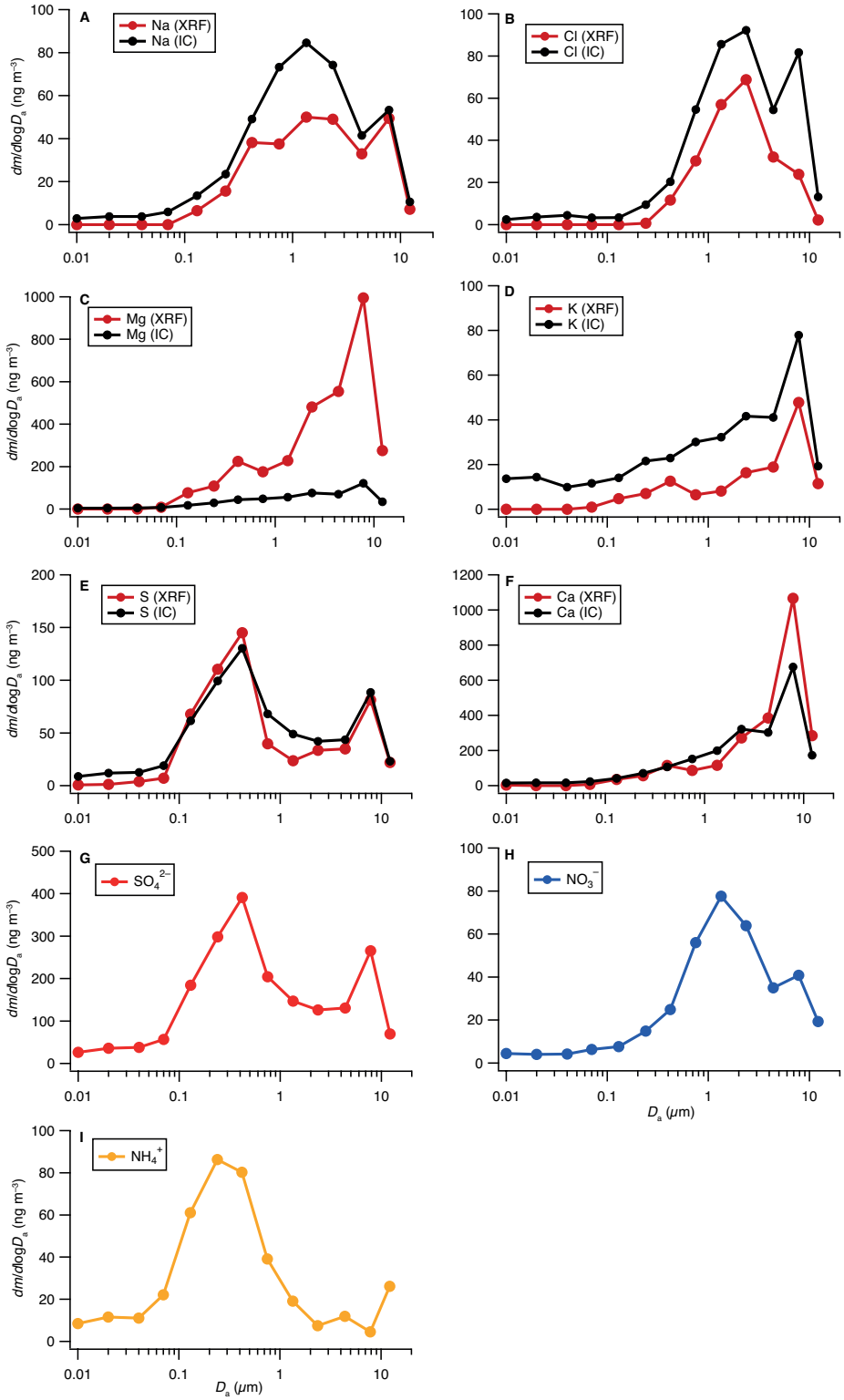

Fig. A3. (**A–F**) Mass size distributions of elements analyzed by XRF (dashed line) and corresponding water-soluble inorganic ions analyzed by IC (solid line). (**G–I**) Mass size distributions of selected ions.

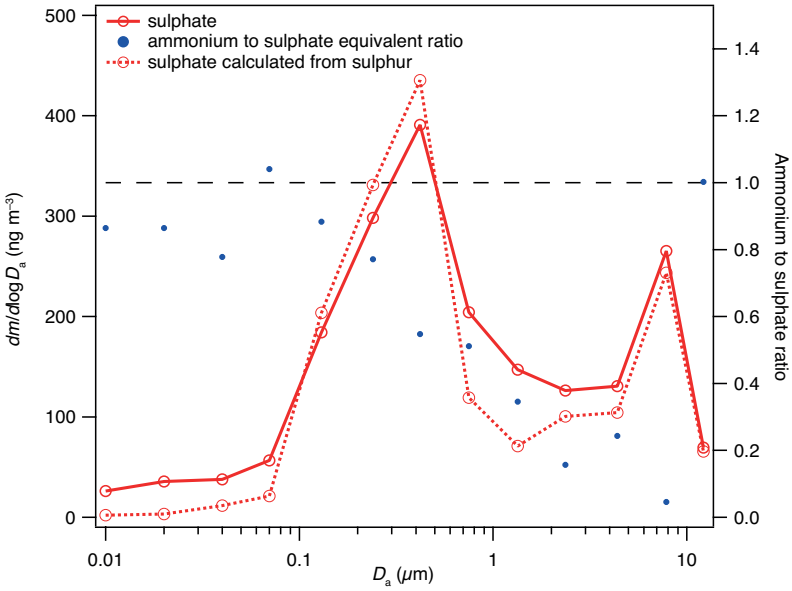

Fig. A4. Ratio of ammonium to sulphate in ion equilents. Calculated sulphate represents the sulphate calculated from EDXRF Sulphur.

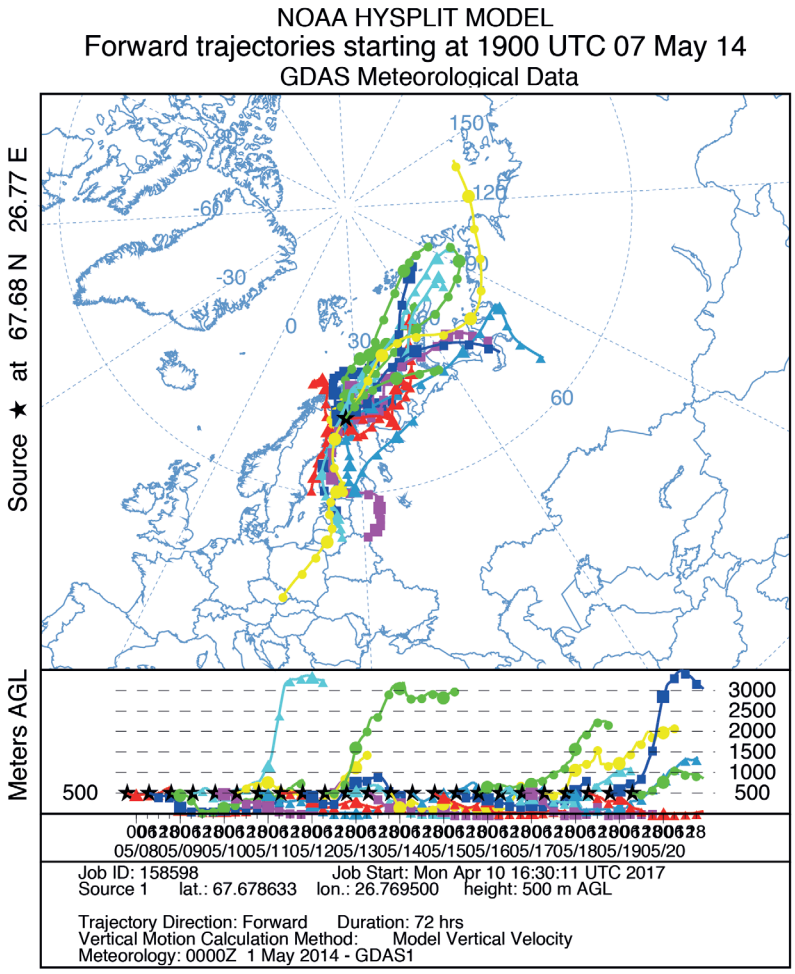

Fig. A5. Air mass back trajectories calculated during the LRT episode indicate that the air mass originated mainly from northeast areas, Siberia and Koala Peninsula.